

## Original articles

Research article

<https://doi.org/10.17308/kcmf.2022.24/9853>

## The effect of the moisture content in benzoic acid on the electrical conductivity of its melts

V. I. Kichigin<sup>1</sup>, I. V. Petukhov<sup>1✉</sup>, A. R. Kornilitsyn<sup>1</sup>, S. S. Mushinsky<sup>2</sup>

<sup>1</sup>Perm State University,  
15 Bukireva str., Perm 614990, Russian Federation

<sup>2</sup>Perm Scientific Industrial Instrument-Making Company,  
106 25th October str., Perm 614990, Russian Federation

### Abstract

The purpose of our study was to analyse the effect of the moisture content in benzoic acid on the electrical conductivity of its melts.

The measurements were performed using impedance spectroscopy in a hermetically sealed metal cell with the temperature of the melts being 160–200 °C. Samples of benzoic acid with different moisture content were used: (i) as-received benzoic acid; (ii) acid dried over anhydrous calcium chloride; (iii) acid exposed to air at 100 % relative humidity.

The study demonstrated that electrical conductivity increased with an increase in the amount of moisture in the acid (the conductivity of the sample with the highest moisture content was about 2.5 times higher than that of the driest sample).

The results obtained are of importance for understanding the mechanisms of proton exchange processes on lithium niobate crystals and can be used for the production of proton-exchange waveguides with stable characteristics.

**Keywords:** Electrical conductivity, Benzoic acid, Melt, Moisture, Proton exchange

**Acknowledgements:** the reported study was supported by the Russian Foundation for Basic Research and by the the Perm Territory, project No. 20-42-596001.

**For citation:** Kichigin V. I., Petukhov I. V., Kornilitsyn A. R., Mushinsky S. S. The effect of the moisture content in benzoic acid on the electrical conductivity of its melts. *Condensed Matter and Interphases*. 2022;24(3): 315–320. <https://doi.org/10.17308/kcmf.2022.24/9853>

**Для цитирования:** Кичигин В. И., Петухов И. В., Корнилицын А. Р., Мушинский С. С. Влияние влажности бензойной кислоты на электропроводность ее расплавов. 2022;24(3): 315–320. <https://doi.org/10.17308/kcmf.2022.24/9853>

✉ Igor V. Petukhov, e-mail: [petukhov-309@yandex.ru](mailto:petukhov-309@yandex.ru)

© Kichigin V. I., Petukhov I. V., Kornilitsyn A. R., Mushinsky S. S., 2022



## 1. Introduction

Benzoic acid (BA) is widely used as a source of protons to perform proton exchange on lithium niobate (LN)  $\text{LiNbO}_3$  crystals in order to produce integrated optical devices. During the proton exchange, a lithium niobate crystal is kept in a BA melt at a temperature of 170–200 °C. During this process, some of the lithium ions in the surface layer of the  $\text{LiNbO}_3$  crystal are replaced with protons:  $\text{LiNbO}_3 + x\text{H}^+ \leftrightarrow \text{H}_x\text{Li}_{1-x}\text{NbO}_3 + x\text{Li}^+$ .

Furthermore, lithium ions in the lithium niobate crystal are replaced with hydrogen ions (protons) followed by the formation of a solid solution  $\text{H}_x\text{Li}_{1-x}\text{NbO}_3$ . This results in an increase in the refractive index of the surface layer of the crystal [1–4]. Due to the increase in the refractive index and the total internal reflection, light travels through the waveguide.

Some researchers believe that it is possible to control the intensity of the proton exchange process by reducing the acidity of the benzoic acid melt with lithium benzoate [5]. We should note that there are very few studies focusing on the state of benzoic acid in the melt. Thus, [6] demonstrates that the concentration of free protons in a benzoic acid melt is considerably low, and the protons required for proton exchange may result from dissociative adsorption of BA molecules in the surface of  $\text{LiNbO}_3$ . Analysis of the IR spectra of benzoic acid melts demonstrated that benzoic acid molecules are mostly present in the melt in the form of dimers [6]. Further studies [7, 8] determined that small amounts of water (about 0.5 wt%) added to benzoic acid intensify the proton exchange process. This could be explained by the increased dissociation of BA and increased concentration of protons in the BA melt. At the same time, only a few studies consider the effect of water added to benzoic acid on the result of proton exchange [9, 10]. Thus, they determined a significant influence of water in a melt of benzoic acid and lithium benzoate on the characteristics of the waveguides formed in lithium niobate [10].

The purpose of our study was to analyse the effect of moisture in benzoic acid on the concentration of free protons in a benzoic acid melt under conditions simulating those of the proton exchange process on lithium niobate. For this purpose, we measured the electrical

conductivity of benzoic acid melts prepared in different ways and with different amounts of water in them.

## 2. Experimental

In our experiments we used benzoic acid prepared in the following ways.

1) As-received benzoic acid (analytical grade) stored in a closed container in a laboratory for 10 months (storage temperature 22–24 °C, the air humidity up to 60 %). This sample will be further on referred to as the BA with the “natural” moisture content.

2) The same BA after drying in a desiccator over calcined calcium chloride for 7 days (dried BA). The weight loss was 0.02 %.

3) The same BA after 5–7 days in a desiccator at 100 % relative air humidity. The weight increase was 0.02 %.

The method used in the experiment was practically the same as the one described in [6]. A hermetic aluminium cell was used (Fig. 1). The cell had two identical metal electrodes embedded in fluoropolymer. The diameter of the electrodes was 5 mm, and the distance between the electrodes was ~ 2 mm. The electrodes were placed parallel to each other. The electrodes were made of either titanium (as in [6]) or aluminium. Before the experiment the electrode surface was polished with fine abrasive cloth and cleaned with ethanol. The lid of the cell had a thermocouple inlet. The cell was sealed to prevent the release of benzoic acid and water vapours during the measurements. The range of operating temperatures  $T$  was 160–200 °C. The accuracy of the maintained operating temperature was  $\pm 1$  °C. The cell was calibrated using 0.01 and 0.02 M solutions of potassium chloride.

Preliminary tests demonstrated that, when kept in BA melts for several hours, titanium and aluminium remain quite stable, and no corrosion products capable of affecting the electrical conductivity of the melt were observed. However, we should note that in the studied temperature range, thin oxide films formed on the surface of Ti and Al in BA melts.

To determine the conductivity of BA melts, we measured the frequency dependences of the impedance of the cell using a Solartron 1287/1255 analyser (Solartron Analytical). The amplitude

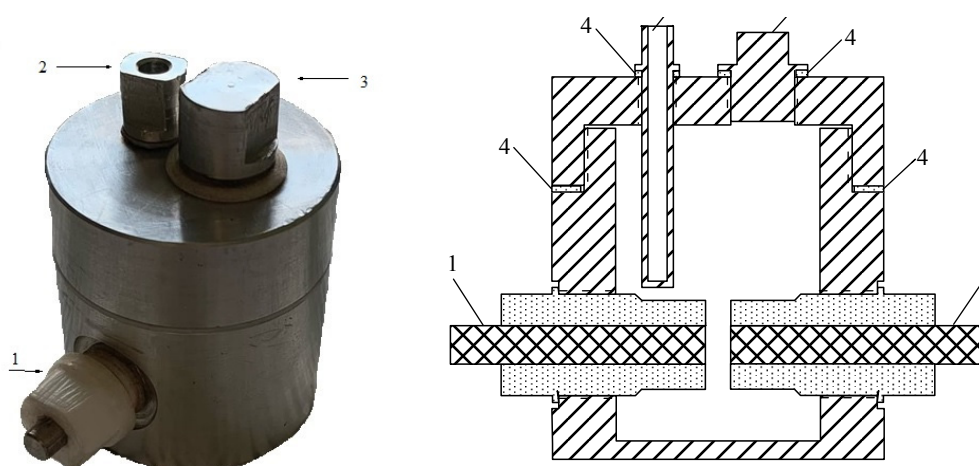


**Fig. 1.** External appearance and cross section of the cell used for conductivity measurements: 1 – titanium or aluminium electrodes; 2 – thermocouple inlet; 3 – plug; 4 – seal ring (fluoropolymer).

of the signal was up to 2 V. Large amplitudes of the alternating signal were used due to the high impedance (up to  $\sim 5 \times 10^7$  Ohm). The resistance of the melt demonstrated a linear current-voltage characteristic. Therefore, a large amplitude signal can be used to reduce the noise in the impedance response [11].

### 3. Results and discussion

Experimental graphs of the impedance spectra on the complex plane are an almost perfect capacitive semicircle with a large diameter and a centre insignificantly displaced from the abscissa (Fig. 2). The semicircle is determined by the electrical resistance of the melt between the electrodes and the geometric capacitance of the measuring cell (not the double-layer capacity on the electrode-melt interface). The explanation for this is provided in [6]. The resistance of the melt is determined by the diameter of the capacitive semicircle (Fig. 2), rather than by the intercept of the capacitive arc on the abscissa at high frequencies  $f$  (when the influence of the geometric capacitance is observed, the real axis intercept at  $f \rightarrow \infty$  practically equals zero).

Geometric capacitance  $C_g = \epsilon_0 \epsilon / d$  ( $\epsilon_0 = 8.854 \times 10^{-12}$ , F/m is the electric constant,  $\epsilon$  is the dielectric constant of the medium filling the cell,  $d$  is the distance between the electrodes) is parallel to series connection of the interfacial impedance and the resistance of the medium between the electrodes [12]. Geometric capacitance has very low values (usually  $10^{-11}$  F [12]) and its impedance  $1/(\omega C_g)$  has high values. However, if the resistance

of the medium between the electrodes and/or the interfacial impedance is high, then the effect of  $C_g$  on the measured impedance of the cell at high frequencies is dominant. Therefore, the effect of  $C_g$  is taken into account when studying high-resistance systems [13–16].

After the measurements in the BA melt (the highest temperature 200 °C) and cleaning the

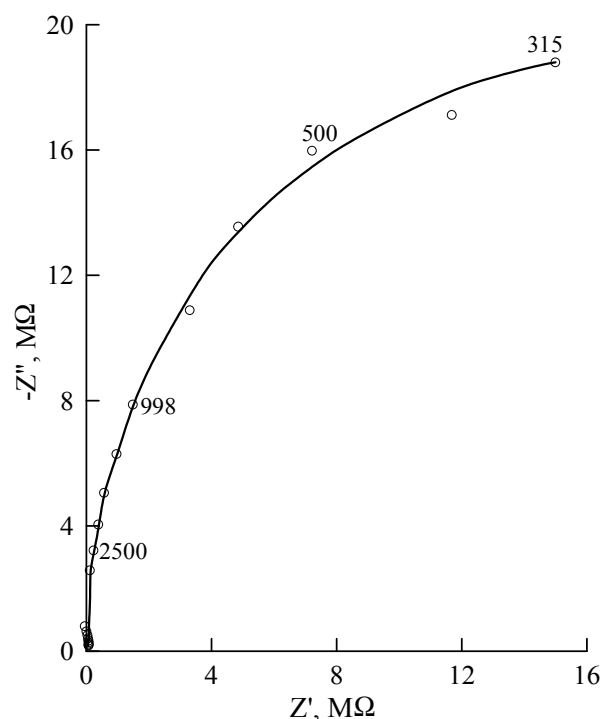


**Fig. 2.** The impedance graph for benzoic acid melt at 190 °C. Benzoic acid was exposed to air at 100 % relative humidity. The numbers next to the symbols are the frequencies in Hz

electrodes from the residues of benzoic acid in isopropyl and ethyl alcohol, the impedance was measured in a 0.02 M KCl aqueous solution with the same geometry of the cell. In this case the measured impedance was determined by the impedance of oxide layers, since the resistance of the solution between the electrodes (about 200 Ohm) was significantly lower than the impedance of the electrode with an oxide film on the surface. The study demonstrated that the diameter of the capacitive arc on the impedance graph of the cell with oxidised electrodes in an aqueous solution at room temperature is by about two orders of magnitude smaller than the diameter of the semicircle on the impedance graph of the cell with the BA melt, even at a higher temperature of the melt. At higher temperatures of the aqueous solution the impedance of the cell with oxidised electrodes reduced. We can thus assume that the difference in the resistance of the melt and the oxide film on the electrode surface at temperatures of 160–200 °C increases (more than two orders of magnitude). This proves that the high impedance of the cell with the BA melt is primarily accounted for by the resistance of the melt between the electrodes, rather than by the oxide film on the electrodes. In accordance with this, the obtained values of the electrical resistance of BA melts did not depend on the material of the electrodes (Ti or Al).

Based on the impedance graph (Fig. 2) we can calculate the capacitance of the cell with a BA melt using the relation [11]  $\omega_m RC = 1$ , where  $\omega_m = 2\pi f_m$ ,  $f_m$  is the characteristic frequency, when the imaginary part of the impedance is maximum, and  $R$  is the resistance determined by the diameter of the semicircle. When  $f_m \approx 315$  Hz,  $R \approx 35$  M $\Omega$  (Fig. 2), we obtain  $C \approx 1.4 \times 10^{-11}$  F, which complies with the geometric capacitance by the order of magnitude. When measured in an aqueous solution of electrolyte with oxidised electrodes (after the experiment with a BA melt), the values of the capacitance obtained based on the impedance graphs vary from several tenths of  $\mu$ F to several  $\mu$ F, i.e. they are noticeably different from the capacitance in the melt.

The results of the measurement of electrical conductivity  $\kappa$  of BA melts in the range of temperatures of 160–200 °C are shown in Fig. 3. Curve 2 agrees well with the  $\log \kappa, 1/T$  dependence

obtained in [6], where as-received benzoic acid was used. When more water is added to BA, the electrical conductivity naturally increases and the slope of  $\log \kappa - 1/T$  lines decreases (Fig. 3). Therefore, the initial moisture content in benzoic acid has a marked effect on the electrical conductivity of the melt. The changes are obviously caused by the presence of H<sub>2</sub>O molecules in the melt. Removal of water from a BA melt can be hindered by the formation of BA-H<sub>2</sub>O complexes [17] followed by their transformations:



where (BH)<sub>2</sub> is a dimer of benzoic acid and BH×H<sub>2</sub>O is a BA-H<sub>2</sub>O complex.

The values of the activation energy  $E_a$  of the ion transfer process in the melt calculated based on the slopes of  $\log \kappa - 1/T$  lines using the formula  $E_a = -2.303Rb$  ( $R$  is the gas constant,  $b$  is the slope), were  $53.3 \pm 6.2$ ,  $39.2 \pm 3.1$  and  $37.6 \pm 5.4$  kJ×mol<sup>-1</sup> for the dried BA, the BA with natural moisture content, and the BA kept at 100 % air humidity respectively. We can see that the two samples of BA containing some moisture have similar values

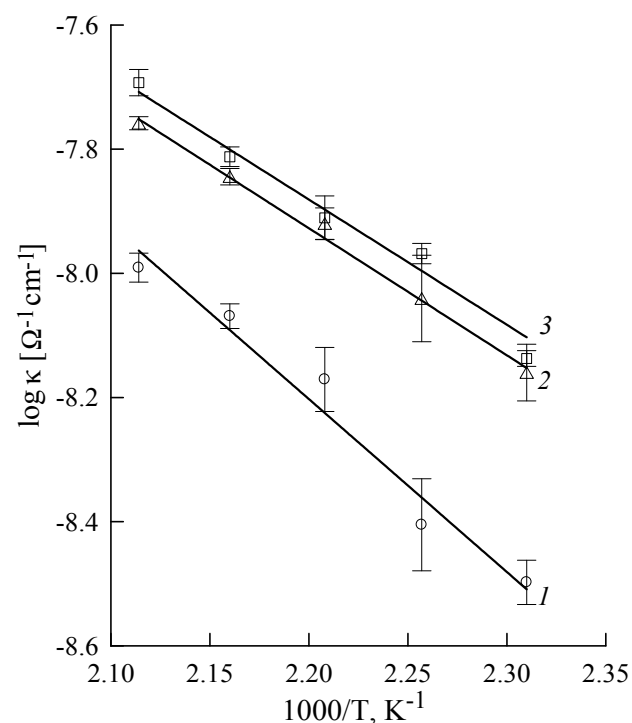


**Fig. 3.** Temperature dependence of electrical conductivity of benzoic acid melts: 1 – dried benzoic acid; 2 – benzoic acid with natural moisture content; 3 – benzoic acid exposed to air at 100 % relative humidity

of  $E_a$ , while  $E_a$  of the dried BA is significantly higher. In moisture containing BA, charge carriers can be formed by reactions (1) and (2). In dried BA, small number of ions is presumably formed according to the autoprotolysis reaction:



The difference in the nature and mechanism of charge carrier generation results in different values of  $E_a$  for moisture containing and dried samples of benzoic acid.

Thus, small amounts of water in benzoic acid melts result in an increase in electrical conductivity. Such an increase may result from a larger number of ions in the melt.

#### 4. Conclusions

The obtained results demonstrate that the effect of moisture in benzoic acid on the electrical conductivity of BA melts and consequently on the concentration of free ions in the melt is noticeable (the sample with the highest moisture content differs from the dried one by 2.5 times at 160 °C), and should be taken into account during the proton exchange process on lithium niobate.

#### Author contributions

All authors made an equivalent contribution to the preparation of the publication.

#### Conflict of interests

The authors declare that they have no known competing financial interests or personal relationships that could have influenced the work reported in this paper.

#### References

1. Korkishko Yu. N., Fedorov V. A. Structural phase diagram of proton-exchange  $\text{H}_x\text{Li}_{1-x}\text{NbO}_3$  waveguides in lithium niobate crystals. *Crystallography Reports*. 1999;44(2): 237–246. Available at: <https://www.elibrary.ru/item.asp?id=13324513>
2. Suchoski P. G., Findakly T. K., Leonberger F. J. Stable low-loss proton-exchanged  $\text{LiNbO}_3$  waveguide devices with no electro-optic degradation. *Optics Letters*. 1988;13(11): 1050–1052. <https://doi.org/10.1364/OL.13.001050>
3. Korkishko Y. N., Fedorov V. A., Feoktistova O. Y.  $\text{LiNbO}_3$  optical waveguide fabrication by high-temperature proton exchange. *Journal of Lightwave Technology*. 2000;18(4): 562–568. <https://doi.org/10.1109/50.838131>
4. Korkishko Yu. N., Fedorov V. A. Structural phase diagram of  $\text{H}_x\text{Li}_{1-x}\text{NbO}_3$  waveguides: the correlation between optical and structural properties. *IEEE Journal of Selected Topics in Quantum Electronics*. 1996;2(2): 187–196. <https://doi.org/10.1109/2944.577359>
5. Korkishko Yu. N., Fedorov V. A., De Micheli M. P., Baldi P. Relationships between structural and optical properties of proton-exchanged waveguides on Z-cut lithium niobate. *Applied Optics*. 1996;35(36): 7056–7060. <https://doi.org/10.1364/AO.35.007056>
6. Kichigin V. I., Petukhov I. V., Mushinskii S. S., Karmanov V. I., Shevtsov D. I. Electrical conductivity and IR spectra of molten benzoic acid. *Russian Journal of Applied Chemistry*. 2011;84(12): 2060–2064. <https://doi.org/10.1134/S1070427211120081>
7. Petukhov I. V., Kichigin V. I., Mushinskii S. S., Minkin A. M., Shevtsov D. I. Effect of water contained in benzoic acid on the proton exchange process, the structure and the properties of proton-exchange waveguides in lithium niobate single crystals. *Condensed Matter and Interphases*. 2012;14(1): 119–123. (In Russ., abstract in Eng.). Available at: <https://www.elibrary.ru/item.asp?id=17711946>
8. Mushinsky S. S., Minkin A. M., Kichigin V. I., Petukhov I. V., Shevtsov D. I., Malinina L. N., Volyntsev A. B., Shur V. Ya. Water effect on proton exchange of X-cut lithium niobate in the melt of benzoic acid. *Ferroelectrics*. 2015;476(1): 84–93. <https://doi.org/10.1080/00150193.2015.998530>
9. Rambu A. P., Apetrei A. M., Dautre F., Tronche H., De Micheli M. P., Tascu S. Analysis of high-index contrast lithium niobate waveguides fabricated by high vacuum proton exchange. *Journal of Lightwave Technology*. 2018;36(13): 2675–2684. <https://doi.org/10.1109/JLT.2018.2822317>
10. Rambu A. P., Apetrei A. M., Tascu S. Role of the high vacuum in the precise control of index contrasts and index profiles of  $\text{LiNbO}_3$  waveguides fabricated by high vacuum proton exchange. *Optics and Laser Technology*. 2019;118: 109–114. <https://doi.org/10.1016/j.optlastec.2019.05.005>
11. Orazem M. E., Tribollet B. *Electrochemical impedance spectroscopy*. Hoboken, New Jersey: John Wiley & Sons, Inc., 2008. 523 p. <https://doi.org/10.1002/9780470381588>
12. Sluyters-Rehbach M. Impedances of electrochemical systems: terminology, nomenclature and representation. Part I: Cells with metal electrodes and liquid solutions (IUPAC Recommendations 1994). *Pure Appl. Chem. IUPAC Standards Online* 1994;66(9) 1831–1891. <https://doi.org/10.1351/pac199466091831>
13. Faidi S. E., Scantlebury J. D. The limitations of the electrochemical impedance technique in the study of electrode reactions occurring in low conductivity media. *Journal of The Electrochemical Society*. 1989;136(4): 990–995. <https://doi.org/10.1149/1.2096898>

14. Yezer B. A., Khair A. S., Sides P. J., Prieve D. C. Use of electrochemical impedance spectroscopy to determine double-layer capacitance in doped nonpolar liquids. *Journal of Colloid and Interface Science*. 2015;449: 2–12. <https://doi.org/10.1016/j.jcis.2014.08.052>

15. SatyanarayanaRaju C. H. S. R. V., Krishnamurthy C. V. Charge migration model for the impedance response of DI water. *AIP Advances*. 2019;9: 035141. <https://doi.org/10.1063/1.5078709>

16. Lensch H., Bastuck M., Baur T., Schütze A., Sauerwald T. Impedance model for a high-temperature ceramic humidity sensor. *Journal of Sensors and Sensor Systems*. 2019;8: 161–169. <https://doi.org/10.5194/jsss-8-161-2019>

17. Schnitzler E. G., Jäger W. The benzoic acid–water complex: a potential atmospheric nucleation precursor studied using microwave spectroscopy and *ab initio* calculations. *Phys. Chem. Chem. Phys.* 2014;16(6): 2305–2314. <https://doi.org/10.1039/c3cp54486a>

## Information about the authors

*Vladimir I. Kichigin*, Cand. Sci. (Chem.), Research Fellow, Research Fellow at the Department of Physical Chemistry, Perm State University (Perm, Russian Federation).

<https://orcid.org/0000-0002-4668-0756>  
kichigin@psu.ru

*Igor V. Petukhov*, Cand. Sci. (Chem.), Associate Professor at the Department of Physical Chemistry, Perm State University (Perm, Russian Federation).

<https://orcid.org/0000-0002-3110-668x>  
petukhov-309@yandex.ru

*Andrey R. Kornilitsyn*, Fourth year student, Faculty of Chemistry; Perm State University (Perm, Russian Federation).

<https://orcid.org/0000-0002-8267-0168>

*Sergey S. Mushinsky*, Head of department, Perm Scientific Industrial Instrument-Making Company (Perm, Russian Federation).

<https://orcid.org/0000-0003-0567-2933>

*Received 04.03.2022; approved after reviewing 13.04.2022; accepted for publication 15.05.2022; published online 25.09.2022.*

*Translated by Yulia Dymant*

*Edited and proofread by Simon Cox*